



Study of De-stratification and Optical Effects Observed During Smoke/Mist Interactions

R. Morlon, P. Boulet and G. Parent, LEMTA, Université de Lorraine, CNRS, UMR 7563, 2 av. de la Forêt de Haye, TSA60604, 54518 Vandoeuvre-lès-Nancy, France*

R. Morlon, S. Lechêne, E. Blanchard, C. Rebuffat and P. Fromy, CSTB - Centre Scientifique et Technique du Bâtiment, 84 avenue Jean Jaurès, Champs sur Marne, 77447 Marne-La-Vallée Cedex 2, France

J. P. Vantelon, Institut P', UPR CNRS 3346 - Département Fluides, Thermique, Combustion – ENSMA, BP 40109 - 86961 Futuroscope Chasseneuil, France

D. Borgiallo, PROFOG, Parc Activité Moulin de Massy, 39 rue du Saule Tapu, 91 300 Massy, France

Received: 25 July 2014/**Accepted:** 4 October 2014

Abstract. This work focuses on interactions between a water mist and a smoke layer generated by a fire. It aims at highlighting and quantifying the mist impact on smoke stratification, investigating both thermal and optical effects. The study is based on large-scale experiments and numerical reconstruction with the computational code fire dynamics simulator (FDS v.6). The use of FDS allows understanding the complicated flow generated by the water mist and the fire, which yields specific gas temperature and opacity conditions within the medium composed of soot and water droplets in suspension. There are two main results. As expected, a de-stratification occurs as a consequence of mist application. A 1 m high smoke-free layer was observed in the present case before mist activation, which disappears due to the mist action. However, consecutive effects on optical and thermal properties are not identical. In the presented tests, water mist application homogenized the gas temperature downward the nozzle location to a value close to 50°C due to both mixing and cooling effects (while temperature was varying between ambient temperature near the floor and 150°C below the ceiling before mist activation). On the contrary opacity measurements revealed remaining discrepancies, in soot and droplet concentrations. Transmissivity decreases after mist activation, but significant variations are still seen in the smoke layer. As a consequence, characterization of the smoke layer with one single technique or the other (namely: opacity measurement or temperature measurement) would lead to different conclusions on the smoke homogeneity. It appears that both measurements should be involved simultaneously for a complete characterization of the environment.

Keywords: Smoke, Water mist, Stratification, Opacity

* Correspondence should be addressed to: P. Boulet, E-mail: pascal.boulet@univ-lorraine.fr

1. Introduction

The usual strategy in France in case of fire is to keep a smoke-free space close to the ground, as long as possible, by using the ventilation systems in particular. This is aimed at first favouring people self-escape and also at warranting good operating conditions for fire-fighting services. While water-based fixed fire fighting systems may interrupt smoke stratification upon which this strategy is based, the regulation allows installing sprinkler systems in buildings for specific cases. For instance, this enables to increase the heat capacity per unit area or to contribute to the fire control. However, such systems can generate significant collateral damages due to the high water flow rate involved, like environmental pollution or material damage. In such context, water mist systems may appear as a good compromise as compared to standard sprinkler systems for the protection of buildings against fire. Indeed, the sprayed droplets are significantly smaller in size (99% of the injected water involves droplets with diameter below 1 mm at one meter from the injection point according to the NFPA and CEN standards) and the corresponding used water flow rate is significantly reduced (according to manufacturers, by a factor at least equal to 10). Moreover, from a scientific point of view, the use of very fine water droplets favours their evaporation, with consecutive benefits for the well-known heat sink effect (which results in a stronger medium cooling) and for the inerting effect of the fire area due to the vapour production which penalizes the fuel-oxygen mixing [1]. In addition to these two effects aimed at fire reduction, water mist also promotes a higher radiation attenuation due to absorption and scattering phenomena, particularly enhanced by a collection of small droplets for a given water quantity. This results in a radiative shielding effect, which was demonstrated through numerical and experimental works (see [2–4], among others).

However, some questions arise regarding the effect of the use of water mist on the smoke stratification and more generally on the interactions between mist, fire and smoke. In the present study focused on water mists (not on sprinkler head sprays), we are studying smoke-mist interactions and the main phenomena are analyzed along a corridor through which smoke flows, with or without perturbation due to a water spray. In that frame, the downward droplet injection by the nozzles results in a drag effect which may alter the smoke flow and may induce a mixing which decreases visibility, escape and safety conditions. Few studies are found on stratification and de-stratification of smoke in case of water mist injection (see Tang et al. [6, 7] or Blanchard [8] among the available studies). At real scale configuration, all above-discussed effects may occur simultaneously, with relative influences depending on various parameters like the droplet size, the water flow rate, the fire itself (heat release rate and fuel type) and the configuration (open or closed space, thermal surroundings, etc.). Blanchard et al. [5] for example studied their respective influences for the specific case of a tunnel at intermediate scale, with water injected through a series of high pressure nozzles (droplets with mean Sauter diameter close to 30 μm). Some similarities may be found with the present problem of smoke flow in a corridor. In both studies, experimentations

were carried out in order to characterize the smoke flow with and without water injection.

Beside the expected observation of stratification alteration due to the mist, one aim of the present study was to provide quantitative information on the changes in the smoke layer when the mist system operates. Temperature distribution and light-obscuring species concentrations are variables directly affected by the smoke flow modification. They were specifically studied here with dedicated measurements and simulations. Temperatures were of course easily measured with standard thermocouples. Light attenuation measurements were used to study changes in the smoke layer distribution. The experimental setup was designed in order to separate the mist/smoke interactions from the other phenomena. The main idea behind the mist injection occurring in the corridor and remote from the fire was to prevent from fire load alteration because of the droplets. On the contrary, the fire and therefore the source of smoke and heat was controlled in a separate room, producing the same incoming smoke flow rate. Only the mist activated in the corridor was supposed to affect the smoke flow. Of course, this configuration takes this study away from a real application where the spray would operate on the fuel, but it warrants that any change in the smoke layer opacity and temperature is only due to the mist action and not attributed to a decrease or change in the fire size.

In present typical tests, the fire is first ignited in a room. After the first stage of fire growth and smoke production increase, it reaches a near stationary regime. The mist system is then activated when the smoke layer is stable under the ceiling, in the neighbouring corridor. Hence, the fire heat release rate (HRR) remains unchanged before and during mist operation. Typically, water mist droplets are expected to cool down the smoke layer (in particular due to their evaporation) and to homogenize the flow in the corridor due to mixing effects. Again, in case of direct mist operation on the fuel, it would not be possible to dissociate whether observed smoke cooling is due to droplet action or to a reduction in the HRR. Similarly, if water mist droplets are involved in the visibility decrease, this must be investigated in keeping the same surrounding conditions, i.e. smoke characteristics, before and during mist activation.

As above mentioned, the main goal of the study is to highlight and to measure the influence of mist spraying on smoke flow, based on two criteria: (i) thermal effect evaluated through temperature profiles and (ii) optical effects based on opacity measurements through transmission data in the visible range. The large-scale tests are accompanied by numerical reconstructions conducted with FDS (fire dynamics simulator—v6). Comparisons are carried out for validation purpose and light-attenuating species or temperature distributions are analysed for a better understanding of the complicated three-dimensional phenomena involved in the smoke flow with and without mist.

2. Experimental Set-Up

2.1. Configuration Description and Fire Load

The real scale setup is composed of a room connected to a corridor via an opened door (see Figure 1). The room has a floor area of 12 m² and is 2.15 m high. The

corridor is 9 m long, 1.4 m wide and 2.35 m high. An opening (90 cm wide by 20 cm high) was created in one wall of the room near the floor to provide make-up air for the fire in order to avoid effects of potential under-ventilation. A 40 cm high lintel was created at one extremity of the corridor in order to get a homogeneous smoke layer thickness.

Tests were conducted with a fire load produced by a 0.09 m² heptane pool in the room (0.3 m × 0.3 m square pool with fuel height of 0.1 m). This liquid fuel was chosen in order to ensure repeatability between experiments, and to reduce uncertainties related to the estimation of the HRR.

2.2. Water Mist System

A real water mist system provided by the manufacturer PROFOG was installed. In the presented tests, a single nozzle (type CEN OH1) operated under water pressure feed 110 bars, corresponding to a flow rate of 27.5 L/min. The nozzle was located in the corridor 3.5 m downward from the corridor's end, on the room side. Very small droplets were sprayed: data provided by the manufacturer indicates that the Sauter diameter is equal to 24 μm at 1 m below the injection point.

2.3. Metrology

2.3.1. HRR Evaluation. The HRR has to be known all along the test, in particular because it will be used as input data in the simulation of the test with the FDS code. The fuel mass loss was monitored with an accuracy evaluated to 1% in the range of interest and was directly related to the HRR through the standard relationship [9].

$$HRR = \eta \cdot \dot{m}_{comb} \cdot h_c \quad (1)$$

where η is the combustion yield for which a value of 0.93 (unitless) was set following a similar work by Blanchard et al. [5], \dot{m}_{comb} (in kg/s) is the used fuel flow rate and h_c (in kJ/kg) stands for the combustion heat for heptane under complete combustion assumption. The steady state HRR of heptanes used in the present application is 44600 kJ/kg.

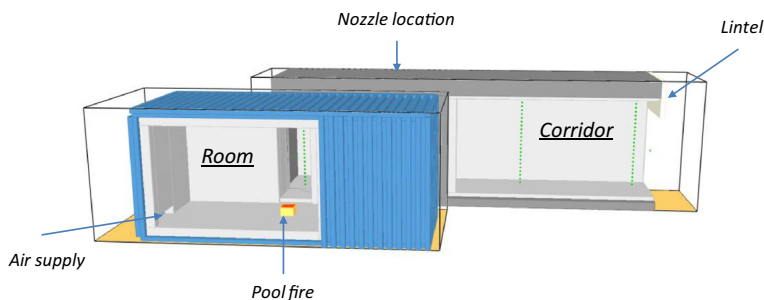


Figure 1. Schematic representation of the "corridor-room" configuration.

Measurement accuracy was checked and repeatability tests were performed during the study, some of which will be presented in the result section for the mass loss and for the temperature.

2.3.2. Temperature Measurement. Home-made K-type thermocouples with bead size 1 mm were used along the corridor to characterize the temperature distribution. The response time appeared sufficient to study the de-stratification effects as we did not look at very short time responses. They are well suited for the temperature range considered in the smoke, with an average uncertainty evaluated to 2.5°C. Three trees involving 18 thermocouples each were set every 3 m in the corridor. They are represented in Figure 2 on a longitudinal view of the corridor, with the connexion to the room on the left hand side. Thermocouples are vertically spaced every 20 cm from the floor up to 1 m, then every 10 cm up to the ceiling.

Thermocouple tree positions will be referred to with labels “1”, “2” and “3” in the result section. Uncertainties will be provided through error bars for the temperatures, based on error analysis and repeatability tests.

2.3.3. Transmissivity Measurements. The transmissivity measurement was based on the attenuation of a laser beam at wavelength 635 nm. The device involved a laser diode used for the beam generation and a detector located at 10 cm from the diode on the line of sight. Laser diodes and detectors were each protected by a small box with a hole for the laser beam path in order to avoid any droplet deposit on the optics. Laboratory tests showed that this device cannot be used with full confidence above 50°C due to thermal perturbations for the device which affect the optical signal. Without mist or before mist system activation, measurements were consequently analysed only in the bottom part of the corridor in the smoke-free area at vertical positions 60 cm, 80 cm and 1 m from the floor (simply allowing to check that smoke is flowing above these heights). During mist

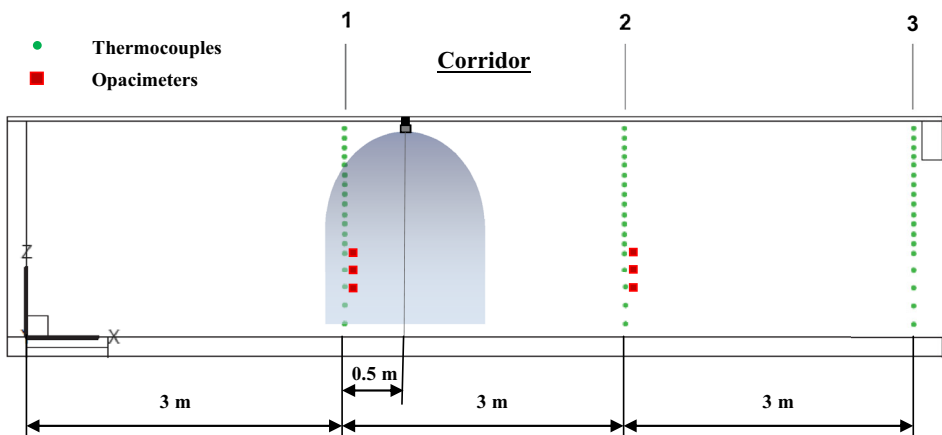


Figure 2. Location of measurement sections within the corridor.

operation, a strong mixing was observed and smoke was dragged through this bottom part but a strong cooling also occurred which allowed using the opacimeters with confidence at all locations (this can be easily checked thanks to simultaneous temperature measurements at the same height, verifying that the local temperature was below 50°C).

The transmissivity was computed as the ratio between the intensity received by the detector and the reference value measured before fire ignition

$$\tau = \frac{I}{I_0} \quad (2)$$

where I_0 and I stand for the signals obtained before ignition and during the fire test, respectively.

The measurement uncertainty is hardly evaluated, but the reliability of the device was checked during several successive heating and cooling steps, demonstrating the stability of the signal registered by the detector located at 10 cm of the source, in the temperature range below 50°C.

3. Numerical Simulations

The present work makes use of fire dynamics simulator (FDS v.6, developed by the NIST, USA) [10]. This 3D CFD tool is widely used in the fire community. It is designed to simulate low-speed, thermally-driven flows. A complete description is provided in [11]. For the present application, it can be recalled that the water mist modelling is based on an Eulerian–Lagrangian approach to simulate the turbulent transport of evaporating droplets. Main parameters defined as input in the simulation are given in Table 1. The geometry of the experimental configuration was reproduced with cubic grid cells of 10 cm × 10 cm × 10 cm. A prescribed HRR curve was set, based on an interpolated piecewise function identified from measurements of the heptane pool mass loss. The FDS fire suppression model was not activated, since water was not sprayed on fire.

The HRR experimental curve was modelled in three steps up to the steady state maximum value of 275 kW reached after 360 s (see Figure 3 without mist and Figure 8 during mist activation). As mist operates in the corridor while the fire is burning in the room, only minor changes in HRR were observed during mist operation, with a discrepancy in the maximum value within the uncertainty range. Possible slight effects were attributed to the air flow from the corridor which can supply a part of the required oxygen to the fire without mist and which was modified after mist activation. It has to be mentioned that Figure 8 could be also analysed considering a slightly higher level of the HRR. Actually, this is due to the fact that the corresponding tests were conducted while the corridor was already heated by several previous tests, rather than to a modification of the HRR regime. The experimental setup was thought to yield the same HRR whether or not the water mist is applied and this assumption was kept in the simulation.

The heptane combustion reaction was defined as follows [8]

Table 1
Main Input Parameters for the Simulation

Dimensions	Room size: 12 m ² Corridor size: 1.4 m large and 9 m long
Boundary conditions	The room is a metallic container covered with resistant mortar cement on the inner face (5 cm in average). Ceiling and walls of corridor are made of cellular concrete (thickness 20 cm) and resistant mortar cement (5 cm in average)
Fire load	Fuel: Heptane C ₇ H ₁₆ Pool surface: 0.09 m ² Soot yield: 0.37 kg/kg CO yield: 0.01 kg/kg
Water mist	Nozzle location: 3.5 m from corridor entrance Injection angle: 120° Droplet size: use of the hybrid Rosin Rammler—log normal law with injected diameter D ₅₀ = 35.5 μm and width of Rosin Rammler distribution Γ = 3 (checked in order to provide the right Sauter diameter of 24 μm and the cumulative volume function provided by the manufacturer, 1 m below the injection point) Activation duration: between 360 s and 660 s Flow rate: 27.5 L/min

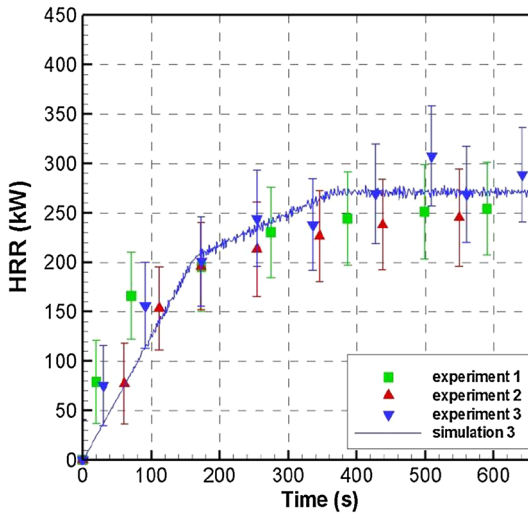
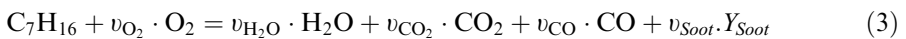


Figure 3. HRR versus time measured in tests without mist (symbols) and piecewise linear function used as input for the simulation (continuous line).



where Y_{Soot} and ν_{Soot} stand for the soot concentration and yield. The other yields ν_i are introduced for the corresponding species I (given in Table 1 for soot and CO).

The temperature distribution comes directly from the simulation. The transmissivity computation when smoke is the only participating species is based on an absorption coefficient evaluated from the soot volumetric fraction following the relationship suggested in [12]

$$\kappa = \frac{5.5 \times f_v}{\lambda} \quad (4)$$

where f_v is the soot volumetric fraction and λ is the radiation wavelength (635 nm for the present application in order to be in agreement with the laser diodes characteristics). Then, the transmissivity was simply computed as

$$\tau = e^{-\kappa L} \quad (5)$$

where L is the smoke layer thickness (10 cm between laser diode and detector when considering the opacimeter configuration). This assumes that no scattering occurs in the medium, which is a reasonable assumption when only soot and gases interact with radiation. Computations in a mixing of smoke and droplets are not yet presented since a simple addition of separated water and soot particles involved in such a Beer's law does not represent the real medium participation (multiple scattering may occur in particular, due to the droplet contribution). However, instead of a numerical transmissivity, soot and droplet distributions can be simply observed in order to explain the transmissivity evolutions, at least qualitatively.

4. Results and Discussion

4.1. Tests Without Water Mist

Three tests were conducted without water mist for a check of the measurement repeatability. The corresponding results are represented with uncertainty limits for HRR and gas temperature results.

4.1.1. Heat Release Rate. The HRR measured in the three tests are represented in Figure 3. A good repeatability is observed between tests: the growing phase and the maximum values are similar. The fire growth lasts around 360s, followed by a stationary step, as above-explained. The error bars represent the confidence intervals around 95% based on variance analysis. The piecewise linear function used for the HRR in the simulation is presented as a continuous line, indicating that the numerical results are based on a representative fire evolution.

4.1.2. Gas Temperature. Figure 4 shows the temperature evolution as a function of time at various vertical positions for the two measurement sections 1 and 2 in the corridor. Experimental data and numerical results are both plotted on the same figures for comparison. Predicted temperatures and measurements are in a satisfactory general agreement. Measured and predicted temperatures follow the

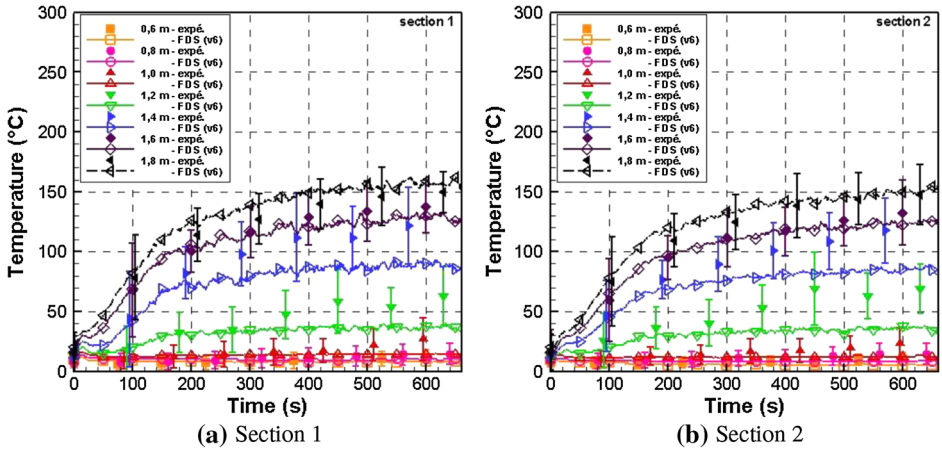


Figure 4. Time-temperature profiles at two locations for tests without mist activation.

HRR evolution: a first fire growth followed by a stationary step. Moreover, predictions stay within the overlapping uncertainty limits based on uncertainties on the measuring chain and considering repeatability tests.

Temperature increase with the vertical position reveals an obvious stratification with a lower part below 1 m above the floor at a near-constant temperature and an upper part above 1 m with the hottest temperatures. Temperature data from sections 1 and 2 are really similar, leading to the observation of a stable smoke layer with a smoke-free height finally evaluated around 1 m.

Instantaneous gas temperature profiles are given on sections 1 and 2 at 355 and 600 s after fire ignition (Figure 5). These profiles confirm that there is an obvious thermal stratification in the corridor. The gas temperature is quite constant below 1 m and quickly rises above this vertical position. Secondly, the FDS code predicts very well the thermal stratification in terms of height of the smoke-free layer. Temperature values are also reasonably well captured. A small discrepancy appears below the ceiling which could be attributed to some uncertainties in the thermal boundary condition (this was ascertained through sensitivity tests carried out varying the insulating properties of the ceiling and the walls, not shown here).

Finally, Figures 4 and 5 confirm that the discrepancy between sections 1 and 2 is really weak, indicating that the smoke layer is stable and homogeneous, with temperature slightly increasing with time.

4.1.3. Transmissivity. The transmissivity variations are first presented as a function of time in Figure 6. Only the predictions by the CFD code are plotted here, since the location of the opacimeters in the bottom part of the corridor i.e. in the smoke-free area leads them to a transmission value equal to 1. Numerically, the stratification which was observed with thermocouples is confirmed through opacity data. The evolution is similar, with a first stage of transmission decrease where temperature was increasing due to the smoke layer development, followed by a

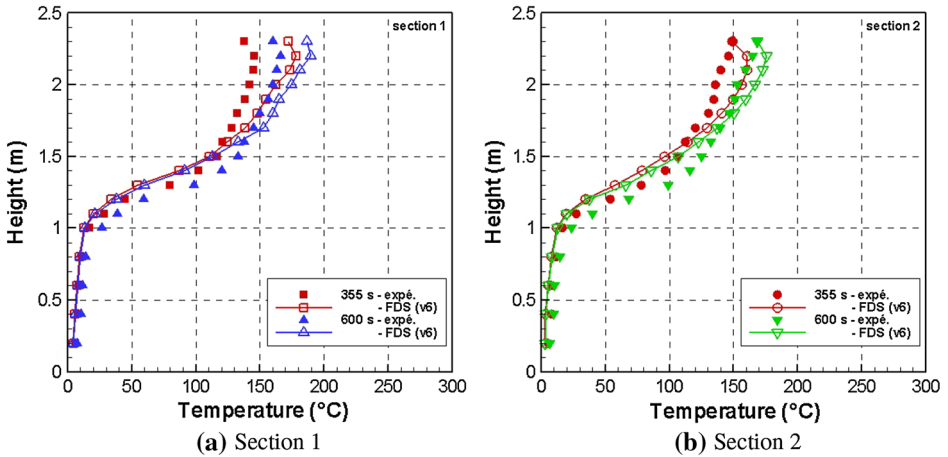


Figure 5. Temperature profiles for tests without mist on two measurement sections at 355 and 600 s.

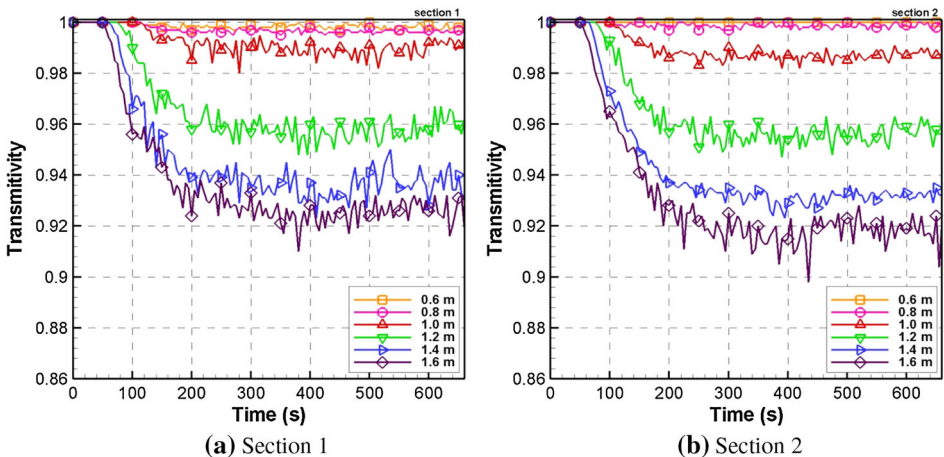


Figure 6. Numerical transmissivity versus time for tests without mist on two measurement sections.

near constant stage when the smoke layer becomes stable, with a transmissivity level depending on the numerical sensor position in the smoke. The bottom part remains free of smoke as confirmed by a transmissivity equal to 1. At 1 m above the floor, the corridor is not strictly smoke-free, but the transmissivity is around 99% and the previous observation of a 1 m high smoke-free layer deduced from temperature data is also reasonable here.

The corresponding transmission profiles are presented at given times, 355 and 600 s after fire ignition as for the gas temperatures in the previous section. In this Figure, experimental data are also plotted with symbols, all almost superimposed

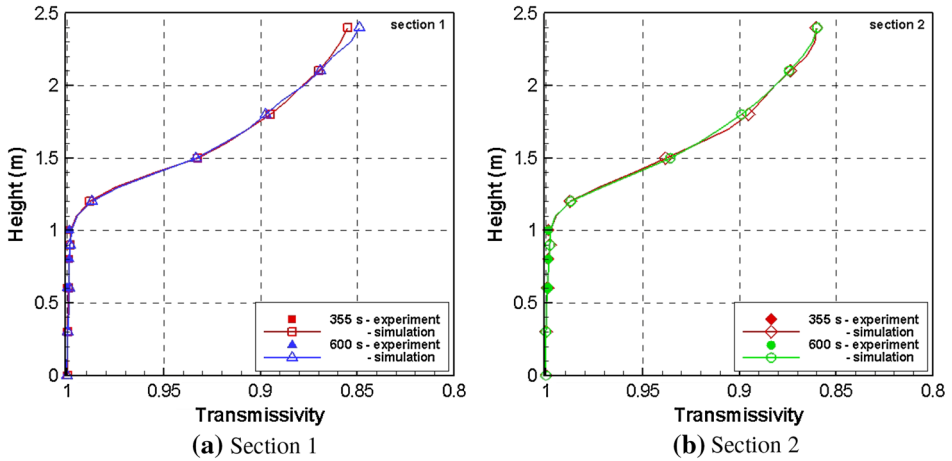


Figure 7. Numerical transmissivity profiles for tests without mist on two measurement sections at 355 and 600 s.

on the left axis, indicating a value close to 1 in the bottom part. As above explained, opacity simulations are in close agreement with temperature data when considering the stratification observation, with a smoke free layer around 1 m above the floor, also confirmed by experimental data in Figure 7.

4.2. Tests with Water Mist

Two repeatability tests have been also conducted in the present case with water mist injection and the corresponding results are used for the uncertainty evaluation in the presented data.

4.2.1. HRR. The HRR evolution is quite the same as for the case without water injection: increase step until 360 s followed by a stationary step despite the water injection between 360 s and 660 s after ignition (Figure 8). As stated above, the HRR is slightly higher because the test was conducted in the corridor already heated by previous tests. This can be understood considering that the higher level is already visible before the mist application, confirming that the mist/smoke interaction is not responsible for that effect. Note that the prescribed HRR is still within the error bars for most of the measurements. This is an important verification in order to allow the comparison of results with and without water injection. Actually, oxygen mainly comes from the opening in the room (which was made for that reason and which is seen to be efficient and to prevent from combustion change while water is injected in the corridor). It confirms that smoke-mist interactions can be studied without fire change, since fire extinguishment is not sought here, the smoke flow is only observed based on optical and thermal criteria.

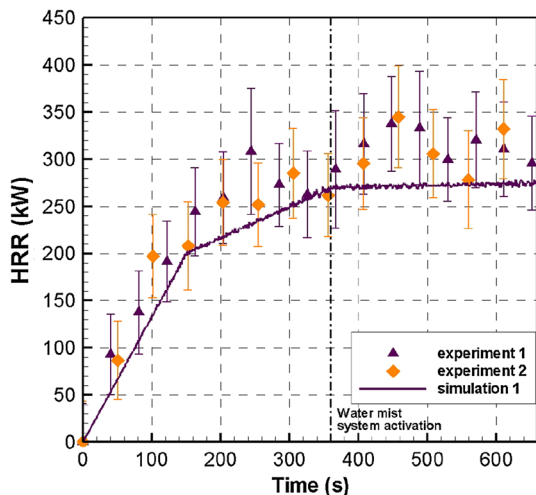


Figure 8. HRR versus time measured in tests involving mist (symbols) and piecewise function used as input for the simulation (line).

4.2.2. Gas Temperature. As explained above, water is injected at 300 s, thanks to a nozzle located 50 cm downstream from the measurement tree of sections 1 and 2. 50 m upstream from section 2. Temperature profiles with time are plotted for both sections in Figure 9. Before mist activation, the increase in temperature is similar to the one observed and commented in Figure 4. The water injection instantaneously results in a sharp perturbation of the temperature distribution, globally leading to a temperature homogenization, even better evidenced in section 2, downstream to the nozzle. It highlights that water injection leads to a strong mixing which causes a de-stratification of smoke. The agreement between experimental and numerical data is satisfactory, with a little discrepancy in section 1 after mist activation.

Comparisons are also presented when focusing on given times for temperature profiles in sections 1 and 2 (see Figure 10). Instantaneous vertical profiles of gas temperature are still in satisfactory agreement, with some discrepancies as compared to the case without mist however. In particular, a discrepancy is observed in section 1 (upstream from the nozzle) in the upper part of the corridor, with a predicted temperature lower than the measured one. Such a cooling could be explained by the droplets injected in this area and possibly by a strong evaporation which would result in a heat sink. The strong smoke/mist interaction and the recirculation loop upstream the mist could be perhaps better described numerically. Beside this singularity, the observed trend confirms a perturbation of the smoke layer, toward a mixing of the smoke due to the water injection. A remaining stratification is observed both numerically and experimentally in the upper part since the fire still produces smoke which flows below the corridor ceiling. The mist activation sharply modifies the profile downstream the nozzle in section 2. The homogenization is also predicted numerically, but a temperature gradient is

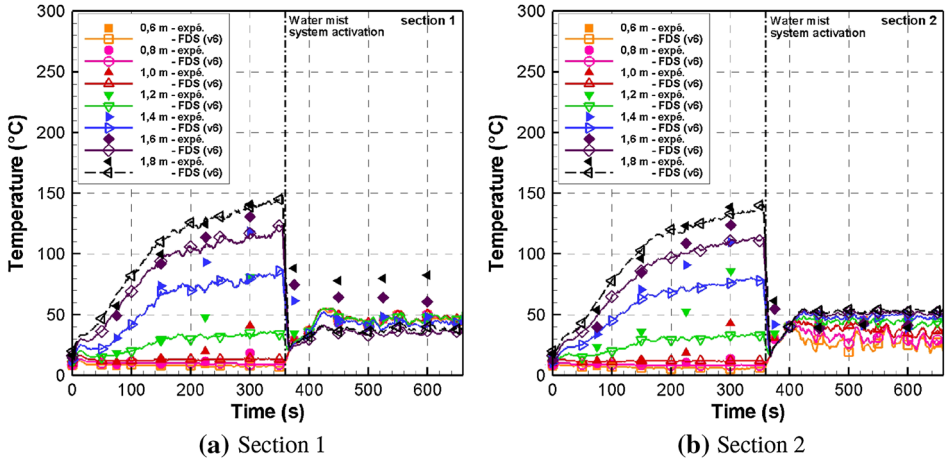


Figure 9. Temperature versus time for tests involving mist on two measurement sections.

still observed, while experimental data show a flat profile. The observation of the velocity profiles shows that the simulation predicts some fresh air entering in the bottom part in a counter flow. Supplementary temperature measurements downward section 2 will check if such air inlet is real in a next campaign. First observation of data at the outlet section (section 3, not shown here) already confirmed that temperature in the lowest part of the outlet section was close to the ambient one. This fresh air backflow is perhaps over-predicted by the simulation. This could be avoided by refining the outflow boundary conditions (not yet tested as a sensitivity test).

Numerically, this is illustrated by Figure 11 which shows the velocity distribution in the central longitudinal plane for the gaseous phase. This figure also shows that the drag effect due to the droplet injection is obvious, while complex loops are induced upstream and downstream the nozzle location. Mixing and cooling effects explain the global homogenization of the temperatures between 40°C and 50°C, still not yet perfectly predicted as above-discussed.

4.2.3. Transmissivity. Transmission data are now provided on the basis of experimental results obtained with the opacimeters solely. The numerical simulation of the transmissivity would require an accurate description of multiple scattering induced by the droplets, which cannot be predicted with relationship (3) and would require the development of a dedicated subroutine which is still beyond the scope of the present study. Data are provided on vertical positions below the initial smoke layer before water injection, which explains the transmission equal to 1 before water mist activation (Figure 12). Then, the above-discussed mixing effect instantaneously decreases the transmission data. Sections 1 and 2 are affected in a different manner due to complex flows induced by the droplets but the smoke-free layer obviously disappears.

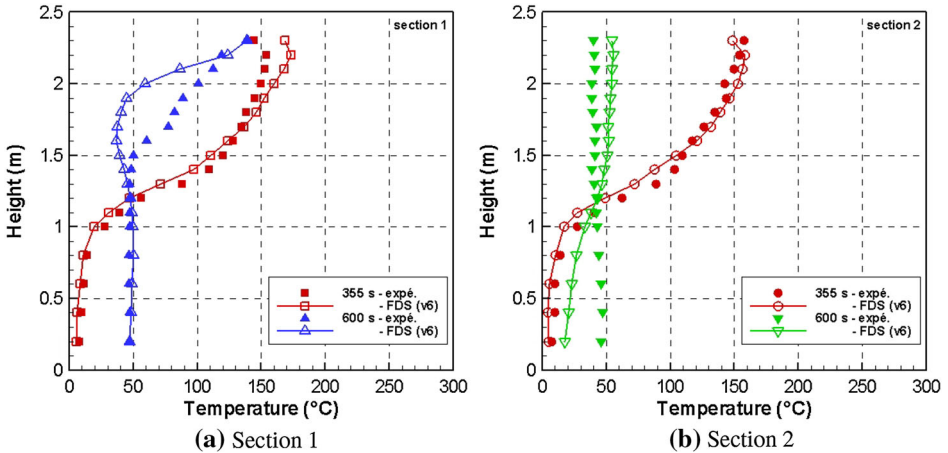


Figure 10. Temperature profiles for tests involving mist on two measurement sections at 355 and 600 s i.e. before and during mist application.

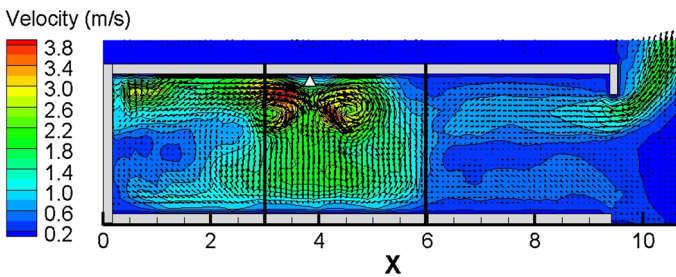


Figure 11. Velocity distribution in a central plane in the corridor, 600 s after ignition and during water injection step.

An interesting observation in section 2, downstream to the nozzle (right plot in Figure 12) is that transmission is even smaller near the floor, than 1 m above the floor. This could be explained by the droplets flowing longitudinally in a higher concentration near the floor. Then, scattering effects would probably result in a weaker transmissivity. This is qualitatively confirmed by the numerical simulation of the droplet concentration in Figure 13, which shows a trend of higher concentration near the floor, but on both sides from the water injection position and not really in section 2 (while it was not expected from transmissivity measurement in Figure 12a and b). Figure 14 also shows the soot concentration which is seen to be quite homogeneous upstream from the nozzle, probably due to the shield effect induced by the droplet flow, while being heterogeneous downstream to the injection point. A higher concentration near the ceiling results from fresh air entering near the floor allowing the smoke to escape only in the upper part.

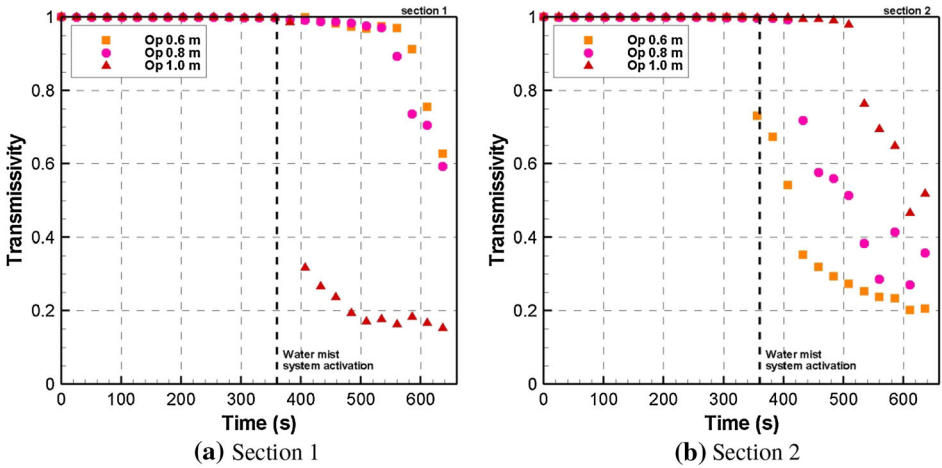


Figure 12. Experimental transmissivity versus time for tests involving mist on two sections.

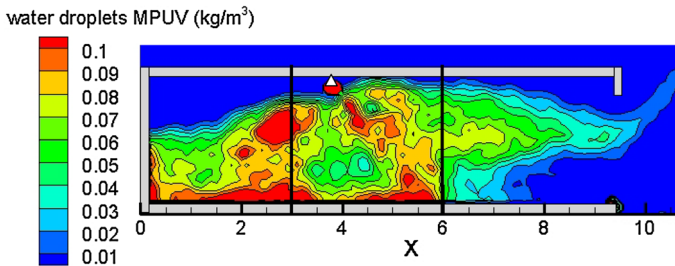


Figure 13. Droplet concentration (Mass Per Unit Volume) in the longitudinal central plane in the corridor, 600 s after ignition.

It is interesting to note that temperature measurements have shown a quite homogeneous behaviour as a function of the vertical position (as a consequence of cooling and mixing effects), while the optical criterion and simulations still show a discrepancy in the species concentrations and the related opacity. Stratification and de-stratification should therefore be considered coupling the different information types. In any case, both methods would show the absence of a smoke-free layer while the mist is activated, but the apparent constant temperature does not show that discrepancies are still found in the species distributions.

5. Discussion of the Results

Phenomena observed when water is sprayed as a mist into a smoke layer during a fire were evidenced and quantified in the present work, considering real scale tests and numerical simulations. Our choice was to make tests carried out in conditions where the fire itself was not directly affected by the water droplets, still burning

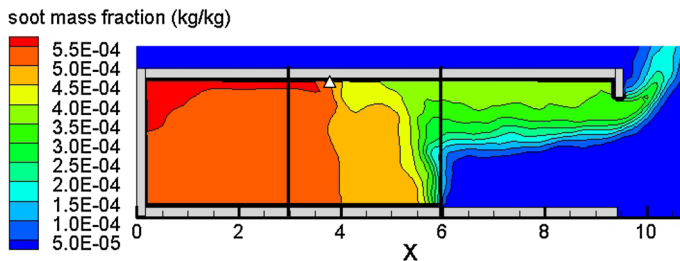


Figure 14. Soot concentration in the longitudinal central plane in the corridor, 600 s after ignition.

with a HRR close to 275 kW. Some similarities may be found with former work by Blanchard et al. [5] who studied the mist action in a tunnel configuration. However, a significantly higher HRR was involved (close to 1500 kW in steady state) and water mist was activated directly on the fire itself (with similar water flow rate 33 L/min and droplet mean Sauter diameter close to 30 μm). Moreover the experimental setup involved a ventilation device which provided a longitudinal velocity around 3 m/s in the tunnel. In Blanchard's study, only temperature profiles were recorded. However, measurements showed a remaining thermal stratification downstream the fire/mist interaction area, while thermal stratification was no more observed experimentally downstream the mist injection point in the present study. Actually, both studies confirm that the mist influence on thermal and optical aspects depends strongly on the fire environment (HRR, air flow, spray characteristics) and the spray characteristics (almost the same droplet size and total water flow rate in both studies but different number of activated nozzles).

Results were also compared with other studies, like the recent one by Tang et al. [6] for example which involved bigger droplets, lower water flow rate and lower operating pressure. By varying the experimental conditions (namely air flow velocity, smoke layer thickness, its temperature, water flow rate), they focused on smoke displacement alteration and internal temperature distribution. They confirmed that spray activation strongly cools down the smoke layer, that the gas temperature remains almost constant with time in the lowest part, while gas temperature is less affected by the spray above the nozzle. They also discussed the effect of increasing the water operation pressure on smoke logging. In the present configuration, the high operation pressure and the consecutive cooling effect could explain the importance of smoke logging.

6. Concluding Remarks

Experiments have been conducted on smoke flowing in a corridor, investigating the de-stratification effect when a water mist was activated. Without spray, a hot and opaque smoke layer was obtained in the upper part of the corridor while a 1 m high smoke-free layer (cool and transparent) was still observed in the bottom part. The numerical simulations carried out with FDS were found to be in a quite

good agreement. Predicted and measured data highlight a smoke layer stable and homogeneous, with temperature slightly increasing with time due to wall heating.

In tests where water was injected in the corridor, instantaneous perturbations were observed. Measurements showed a strong cooling and a fast homogenization of the temperature distribution downward the spray. This effect was explained by cooling due to heat transfer between droplets and gas and by mixing of the smoke layer with fresher air within the environment. In addition to this phenomenon often highlighted in previous researches, the present work shows that this homogenization is not extendable to optical aspects. Indeed, measurements of transmission differ strongly along the vertical axis: it can be smaller near the floor than 1 m above the floor. Thus, measurements demonstrated that thermal and optical environments are found partly decoupled during mist application. Numerical reconstructions gave a possible explanation for this observation. Droplets were predicted flowing longitudinally in a higher concentration near the floor and predicted species concentrations (droplet and soot concentrations in particular) revealed some concentration discrepancies in the smoke-droplet flow.

Concerning the capability of the computational tool to estimate the conditions during mist operation, physical trends were captured qualitatively. In more details, gas temperatures were found in satisfactory agreement but with higher discrepancies in spray injection surroundings.

Our work will be extended examining stratification and de-stratification effects in connection with mist-smoke interactions, varying the experimental conditions: HRR, spraying conditions and mist characteristics (droplet size, flow rate).

Finally, the present work demonstrates the necessity to involve both thermal and optical measurements when spray system is activated in order to be able to characterize the environment. In other words, the use of one single technique could affect the conclusions regarding the smoke flow. Moreover, these optical and thermal criteria could be even completed by toxicity measurements for a third method of stratification characterization.

References

1. Jenft A, Collin A, Boulet P, Pianet G, Breton A, Muller A (2014) Experimental and numerical study of pool fire suppression using water mist. *Fire Saf J* 67:1–12
2. Collin A, Lechêne S, Boulet P, Parent G (2010) Water mist and radiation interactions—application to a water curtain used as a radiative shield. *Numer Heat Transf A* 57:537–553
3. Lechêne S, Acem Z, Parent G, Jeandel G, Boulet P (2011) Upward vs downward injection of droplets for the optimization of a radiative shield. *Int J Heat Mass Transf* 54:1689–1697
4. Lechêne S, Acem Z, Parent G, Collin A, Boulet P (2012) Radiative shielding by water mist: comparison between downward, upward and impacting of droplets. *J Phys* 369:012027
5. Blanchard E, Boulet P, Fromy P, Desanghère S, Carlotti P, Vantelon JP, Garo JP (2014) Experimental and numerical study of the interaction between water mist and fire in an intermediate test tunnel. *Fire Technol* 50(3):565–587

6. Tang Z, Fang Z, Yuan JP, Merci B (2013) Experimental study of the downward displacement of fire-induced smoke by water sprays. *Fire Saf J* 55:35–49
7. Tang Z, Vierendeels J, Fang Z, Merci B (2013) Description and application of an analytical model to quantify downward smoke displacement caused by water spray. *Fire Saf J* 55:50–60
8. Blanchard E (2011) Modélisation de l'interaction entre brouillard d'eau et feu en tunnel. PhD Thesis, Université Henri Poincaré Nancy 1
9. Babrauskas V (2002) Heat release rates (Chap. 3). In: *SFPE Handbook of fire protection engineering*, 3rd edn. SFPE, New England, pp 3–37
10. McGrattan K, McDermott R, Hostikka S, Floyd J (2013) FDS (Version 6) user's guide. Technical report, NIST
11. McGrattan K, McDermott R, Hostikka S, Floyd J (2013) FDS (Version 6) Technical reference guide: mathematical model, vol 1. Technical report, NIST
12. Solovjov VP, Webb BW (2001) An efficient method for modeling radiative transfer in multicomponent gas mixtures with soot. *J Heat Transf* 123:450